The plasmaspheric plume and magnetopause reconnection

B. M. Walsh[1], T. D. Phan[2], D. G. Sibeck[1], and V. M. Souza[1,3]

B. M. Walsh, Heliospheric Division, NASA Goddard Space Flight Center, Greenbelt, Maryland, USA. (brian.walsh@nasa.gov)

D. G. Sibeck, Heliospheric Division, NASA Goddard Space Flight Center, Greenbelt, Maryland, USA.

T. D. Phan, University of California, Berkeley, California, USA.

V. M. Souza, National Institute for Space Research/INPE, Sao Jose dos Campos, Brazil.

[1]NASA Goddard Space Flight Center,
Greenbelt, Maryland, USA.

[2]University of California, Berkeley,
California, USA.

[3]National Institute for Space
Research/INPE, Sao Jose dos Campos,
Brazil.

We present near-simultaneous measurements from two THEMIS spacecraft at the dayside magnetopause with a 1.5 hour separation in local time. One spacecraft observes a high density plasmaspheric plume while the other does not. Both spacecraft observe signatures of magnetic reconnection, providing a test for the changes to reconnection in local time along the magnetopause as well as the impact of high densities on the reconnection process. When the plume is present and the magnetospheric density exceeds that in the magnetosheath, the reconnection jet velocity decreases, the density within the jet increases, and the location of the faster jet is primarily on field lines with magnetosheath orientation. Slower jet velocities indicate reconnection is occurring less efficiently. In the localized region where the plume contacts the magnetopause the high density plume may impede the solar wind-magnetosphere coupling by mass-loading the reconnection site.

1. Introduction

It has been predicted that solar wind-magnetospheric coupling is limited during times when dense plasmaspheric plumes contact the dayside magnetopause. These predictions are based on theory and modeling which show that the reconnection rate decreases when the plasma density increases [e.g. *Cassak and Shay*, 2007; *Birn et al.*, 2008]. As the plume contacts the magnetopause it should mass-load the region and slow magnetopause reconnection. This in turn should decrease the level of solar wind-magnetosphere coupling.

Observationally, the control of solar wind-magnetospheric coupling by the plume has been inferred in statistical work by *Borovsky and Denton* [2006]. *Borovsky and Denton* [2006] examined many years of solar wind measurements and geosychronous plume observations to show reduced solar wind-magnetospheric coupling as measured through geomagnetic indices. Global MHD modeling shows that mass-loading of the magnetopause reconnection will greatly slow the reconnection rate in a localized region, which is consistent with previous results [*Borovsky et al.*, 2008].

Although many measurements of the plume exist at geosynchronous orbit [e.g *Moldwin et al.*, 1994; *Elphic et al.*, 1996; *Borovsky and Denton*, 2008], few spacecraft measurements have been reported of the plume actually contacting the magnetopause [e.g *Su et al.*, 2000; *McFadden et al.*, 2008; *Walsh et al.*, 2013]. The current study provides simultaneous spacecraft observations at the magnetopause with a separation in local time. One spacecraft observes a high density plume contacting the magnetopause near local noon while another spacecraft encounters the magnetopause prenoon and does not observe the plume. Several studies have presented cases with multiple spacecraft observing reconnec-

tion at the magnetopause with local time separation [*Phan et al.*, 2000; *Dunlop et al.*, 2011], but this is the first involving the plume. Since the magnetosheath properties are roughly the same at the two spacecraft, the observations serve as a test for the impact of the plume on magnetopause reconnection and solar wind-magnetosphere coupling.

2. Instrumentation

In-situ observations from the THEMIS spacecraft are used. Magnetic field measurements are made with the fluxgate magnetometer (FGM) [*Auster et al.*, 2008]. Onboard plasma moments (MOM) from the ESA instrument [*McFadden et al.*, 2008] are used for bulk flow velocities, and energetic particle measurements are obtained from the Solid State Telescope (SST). The electron density measurements come from the spacecraft potential measured by EFI [*Bonnell et al.*, 2008], since much of the cold plasmaspheric population is below the energy threshold of ESA (∼8 eV).

3. Observations

During a 45 minute interval from 13:10-13:55 UT on 15 Sept 2008, both ThA and ThD cross the magnetopause a number of times. The spacecraft are primarily equatorial and are separated by 1.5 h in MLT at 11.6 h and 10.0 h respectively. The locations of the spacecraft are shown in Figure 1.

Figure 2 presents solar wind observations from ThB which is located just upstream of the bow shock at GSM (X,Y,Z) = (26, -13, 3) R_E. The IMF Bz component remains southward for the entire interval with the exception of several short periods near 1341UT. For much of the interval the IMF clock angle ($CA = tan^{-1}(\frac{By}{Bz})$) is greater than 120°. The magnetic field strength and electron density remain nearly constant during this interval

indicating steady inputs to the magnetopause. Propagation time of the measurements from the upstream spacecraft (ThB) to the subsolar magnetopause is estimated at less than 13 minutes based on the bulk flow velocity.

Figure 3 shows the measurements from ThA and ThD during the same time period while each encounters the magnetopause. Both spacecraft measure the electron density in the magnetosheath to be ∼5-10 cm^{-3}, however the density measured inside the magnetosphere by the two spacecraft differs by two orders of magnitude. Inside the magnetosphere ThD observes a density of 0.4-0.7 cm^{-3}, typical for the dayside outer magnetosphere. ThA measures the density of the plume plasma contacting the magnetopause to be 18-72 cm^{-3}. The magnetic field and velocity measurements are presented in the boundary normal coordinate system (LMN) where L is along the outflow direction, M is along the X-line, and N is the current sheet normal. The coordinate system was identified through minimum variance of the magnetic field (MVAB) [*Sonnerup and Cahill*, 1967]. The spacecraft observe jets or enhancements in the v_L component in both the positive and negative direction while encountering the boundary layer. This indicates the spacecraft were making observations both above and below the reconnection site as seen by *Trenchi et al.* [2008].

We attribute the difference in density between the two spacecraft to be from a localized plasmaspheric plume given the magnitude of the density and the location of the observations. A number of studies have demonstrated a connection between the plasmaspheric structure and geomagnetic activity [e.g *Chappell et al.*, 1970; *Higel and Lei*, 1984; *Carpenter et al.*, 1993]. During geomagneticly disturbed periods the plasmapause erodes radially

inward and a drainage plume can form in the dusk sector extending sunward towards the magnetopause [*Spasojević et al.*, 2003]. The current event is consistent with this picture as it occurs during a moderate geomagnetic storm with a Sym-H index of -40 nT. During this time period the enhanced magnetospheric convection brings the plasmaspheric plume to the magnetopause where it is observed by one of the two spacecraft at the boundary.

4. Reconnection

During the time period from 13:10-13:55 UT both spacecraft experience a number of full and partial magnetopause crossings. For closer analysis of the structure of reconnection we select full magnetopause crossings with reconnection occurring. We identify full crossings by a the rotation of the magnetic field and a change in density. For a rotational discontinuity at the magnetopause, MHD predicts the outflow will be Alfvènic in the reference frame of the X-line. In the case of asymmetric reconnection the Alfvén speed is a hybrid of the Alfvén speed on each side of the current sheet. A 15 s time period just inside and outside the magnetopause is averaged to obtain the plasma parameters in the magnetosphere and magnetosheath. Reconnection during these crossings is identified when the jet speed is within 25% of the predicted hybrid Alfvén velocity from *Cassak and Shay* [2007]. The jet velocities are obtained by subtracting the reconnecting component of the exhaust velocity (v_L) from the background flow in the L direction. The exhaust velocity is selected as the maximum value within the current sheet.

The background flow is taken from the side with the larger mass inflow which is determined from ρ/B following *Cassak and Shay* [2007]. The ratio of mass inflow for each crossing is given in Table 1 with the assumption that the effective mass is similar for

the plasma on both sides of the magnetopause. At ThD the magnetosheath mass inflow clearly dominates and subtracting the background v_L from the magnetosheath is a clear choice. At ThA the magnetospheric mass inflow is larger but does not dominate. In this scenario it is likely both sides are contributing plasma, so the decision it is less clear. Since we are only selecting one side to subtract a background, we choose the side with the larger mass inflow. In these crossings v_L from the magnetosheath is subtracted when no plume is present (ThD), while v_L from the magnetosphere is subtracted when the plume is present (ThA). We note however that our criteria for reconnection is met using v_L from either side of the boundary.

Using the crossing by ThD at 13:34UT as an example, the maximum v_L component within the exhaust is 370 km/s while the background component (magnetosheath in this case) is 8 km/s. This gives a jet velocity of $v_{jet} = v_{exhaust}$ - $v_{background} = 362$ km/s. The hybrid Alfvén speed is 364 km/s, so the jet measurement is 99% of the predicted value and is therefore selected as a reconnection event. With these criteria, we've identified three periods for each spacecraft when reconnection is observed during a full magnetopause crossing. The times of these periods and reconnection parameters are provided in Table 1. The times are also shown in Figure 3 with black arrows. We note that the derivation of the hybrid Alfvén velocity from *Cassak and Shay* [2007] assumes $v_L = 0$ km/s on both sides of the current sheet which does not occur in these measurements. The background flow is subtracted from the exhaust measurement to obtain an appropriate reference frame for comparison with the prediction.

Two near simultaneous crossings from ThA and ThD are shown in Figure 4 for closer analysis. These are representative of the other crossings by each spacecraft. In this example ThA crosses the magnetopause from the magnetosheath to the magnetosphere at 13:31:37UT. Three minutes later ThD passes from the magnetosphere to the magnetosheath at 13:34:45UT. ThD measures a density of 0.2 cm^{-3} inside the magnetosphere while ThA measures a magnetospheric density of 55 cm^{-3} (panels b and f of Figure 4). Part of the cold plume plasma can be seen as a flux enhancement in the ion energy spectragram with an energy near 10 eV (Figure 4e). This cold population coexists with the hotter magnetospheric population observed by both spacecraft.

The density asymmetry between the spacecraft impacts several aspects of the reconnection. The first aspect is the location of the reconnection jet in respect to the X-line. In the case of ThD, the density is higher in the magnetosheath resulting in asymmetric reconnection where the jet lies primarily on magnetic field lines with magnetospheric orientation ($+B_L$) (Figure 4c,d). This is typical for terrestrial magnetopause reconnection. ThA observes a higher density in the magnetosphere causing the reverse asymmetry. In this scenario the jet lies primarily on magnetic field lines of magnetosheath orientation ($-B_L$) or lower density (Figure 4g,h). In each case the jet is displaced towards the side with lower density and lower ρ/B, consistent with predictions by MHD theory [*Cassak and Shay*, 2007]. The magnetic field orientation during the peak jet velocity for the other crossings is consistent with what each spacecraft observes in this example and is included in Table 1.

The magnitude of the jet velocities are also different between the spacecraft (Figure 4c, g). ThD observes a significantly larger jet velocity (v_{jet}=362 km/s) than ThA (v_{jet}=162 km/s). ThD also observes lower density inside the magnetopause than ThA. The jet is caused by the magnetic curvature force that accelerates the exhaust plasma to the hybrid Alfvén speed. The Alfvén speed is inversely proportional to $n^{1/2}$, so a slower jet velocity in the crossings with higher density is consistent with the observations. In addition to the velocity, the density within each exhaust jet is also different in the two cases. The density shows mixing of the plasma populations from both sides. In the case of ThA, when reconnection is highly asymmetric, the bulk of the contribution comes from the the magnetosheath side or the side with larger density. The velocity and density within each jet are given in Table 1.

5. Discussion

A predicted effect of the plasmaspheric plume at the magnetopause is that the dense plasma in the magnetosphere will slow reconnection and decrease solar wind-magnetospheric coupling [*Borovsky and Denton*, 2006]. Theory of symmetric [*Sweet*, 1958] as well as asymmetric reconnection [*Cassak and Shay*, 2007] show the reconnection rate to scale with the Alfvén speed or inversely with $n^{1/2}$. As the density increases the reconnection rate decreases. The multispacecraft observations presented here show reconnection occurring over a range of local time with similar magnetosheath but greatly different magnetospheric densities.

With current spacecraft instrumentation, observational measurements of a dimensionless reconnection rate can vary by a factor of 2 or more for a single event depending on

what techniques are used [*Phan et al.*, 2001]. These techniques often require identifying a boundary normal of the current sheet which can be done through several methods, as well as identifying the velocity of the X-line structure under an assumption of constant motion. Both of these can introduce significant errors into the measurement. An alternative way to measure the efficiency of reconnection is to monitor the velocity of the exhaust jet. Although it doesn't produce a rate quantitatively similar to other methods (i.e. $B_n/|B|$ or v_n/v_A), the efficiency of reconnection at two spacecraft can be compared by the magnitude of the reconnection jet. Using the jet velocity assumes the dimensionless reconnection rate stays roughly constant over the time period of the spacecraft pass. If the reconnection rate does not change significantly, the velocity of the jet is a function of the inflow speed which is in turn a measure of the reconnection rate.

ThD observes faster jets attending crossings without a plume than ThA observes with a plume. This is consistent with the idea that the reconnection rate decreases with higher densities and that the plasmaspheric plume can slow reconnection when it contacts the magnetopause. On a larger scale these observations show that reconnection will be impacted in a localized region where the plume contacts the magnetopause. The size of the plume at the magnetopause must also determine the impact on the overall solar wind-magnetosphere coupling, and a measure of this size is needed to quantify this effect. In addition to affecting reconnection, the newly opened field lines will transport plasmaspheric plasma as they convect over the poles to the nightside where the plasma is deposited into the tail and lobes [*Elphic et al.*, 1997]. To understand the global impact of the plume on solar wind-magnetospheric coupling, one must follow the entire circula-

tion pattern beginning with the entrainment of dense plasmaspheric material on newly reconnected magnetic field lines.

6. Conclusion

Near-simultaneous spacecraft observations at the magnetopause shows the presence of a localized region with high densities from the plasmaspheric plume. Separated by 1.5 hours in magnetic local time, both spacecraft measure magnetic reconnection, however only one measures the high density plume. When the plume is present the reconnection jets have lower velocities and larger densities. A decreased jet velocity indicates a localized reduction in solar wind-magnetosphere coupling due to the presence of the plasmaspheric plume. These observations also show that the properties of reconnection are a function of the local plasma density and vary along the surface of the magnetopause.

Acknowledgments. The authors would like to thank L. Wilson for useful discussions. Support was given by the National Science Foundation through grant AGS-1136827. We acknowledge NASA contract NAS5-02099 and instrument teams for use of the data from the THEMIS Mission, Specifically: C. W. Carlson and J. P. McFadden for use of ESA data, J. W. Bonnell and F. S. Mozer for use of EFI data, and K. H. Glassmeier, U. Auster and W. Baumjohann for the use of FGM data.

References

Auster, H. U., et al. (2008), The THEMIS fluxgate magnetometer, *Space Sci. Rev., 141*, 235-264.

Birn, J., J.E. Borovsky, and M. Hesse (2008), Properties of asymmetric magnetic reconnection, *Phys. Plasmas, 15*, 032101, doi:10.1063/1.2888491.

Bonnell, J. W., F. S. Mozer, G. T. Delory, A. J. Hull, R. E. Ergun, C. M., Cully, V. Angelopoulos, and P. R. Harvey (2008), The Electric Field Instrument (EFI) for THEMIS, *Space Sci. Rev., 141*, 303-341, doi:10.1007/s11214-008-9469-2.

Borovsky, J. E., and M. H. Denton (2006), Effect of plasmaspheric drainage plumes on solar-wind/magnetosphere coupling, *Geophys. Res. Lett.*, *33*, L20101, doi:10.1029/2006GL026519.

Borovsky, J. E., and M. H. Denton (2008), A statistical look at plasmaspheric drainage plumes,*J. Geophys. Res.*, *113*, A09221, doi:10.1029/2007JA012994.

Borovsky, J. E., M. Hesse, J. Birn, and M. M. Kuznetsova (2008), What determines the reconnection rate at the dayside magnetosphere?, *J. Geophys. Res.*, *113*, A07210, doi:10.1029/2007JA012645.

Carpenter, D. L., B. L. Giles, C. R. Chappell, P. M. E. Decreau, R. R. Anderson, A. M. Persoon, A. J. Smith, Y. Corcuff, and P. Canu (1993), Plasmasphere dynamics in the duskside bulge region: A new look at an old topic, *J. Geophys. Res.*, *98*(A11), 19243–19271, doi:10.1029/93JA00922.

Cassak, P. A., and M. A. Shay (2007), Scaling of asymmetric magnetic reconnection: General theory and collisional simulations, *Phys. Plasmas*, *14*(10), 102114, doi:10.1063/1.2795630.

Chappell, C. R., K. K. Harris, and G. W. Sharp (1970), A study of the influence of magnetic activity on the location of the plasmapause as measured by OGO 5, *J. Geophys.*

Res., *75*(1), 5056, doi:10.1029/JA075i001p00050.

Dunlop, M. W., et al. (2011), Extended magnetic reconnection across the dayside magnetopause, *Phys. Rev. Lett.*, *107*, 025004, doi:10.1103/PhysRevLett.107.025004.

Elphic, R. C., L. A. Weiss, M. F. Thomsen, D. J. McComas, and M. B. Moldwin (1996), Evolution of plasmaspheric ions at geosynchronous orbit during times of high geomagnetic activity, *Geophys. Res. Lett.*, *23*(16), 21892192, doi:10.1029/96GL02085.

Elphic, R. C., M. F. Thomsen, and J. E. Borovsky (1997), The fate of the outer plasmasphere, *Geophys. Res. Lett.*, *24*(4), 365368, doi:10.1029/97GL00141.

Higel, B., and W. Lei (1984), Electron density and plasmapause characteristics at 6.6 RE: A statistical study of the GEOS 2 relaxation sounder data, *J. Geophys. Res.*, *89*(A3), 1583-1601, doi:10.1029/JA089iA03p01583.

McFadden, J. P., C. W. Carlson, D. Larson, J. Bonnell, F. S. Mozer, V. Angelopoulos, K.-H. Glassmeier, and U. Auster (2008), Structure of plasmaspheric plumes and their participation in magnetopause reconnection: First results from THEMIS, *Geophys. Res. Lett.*, *35*, L17S10, doi:10.1029/2008GL033677.

McFadden, J. P., C. W. Carlson, D. Larson, M. Ludlam, R. Abiad, B. Elliott, P. Turin, M. Marckwordt, and V. Angelopoulos (2008), The THEMIS ESA plasma instrument and in-flight calibration, *Space Sci. Rev., 141*, 277-302, doi:10.1007/s11214-008-9440-2.

Moldwin, M. B., M. F. Thomsen, S. J. Bame, D. J. McComas, and K. R. Moore (1994), An examination of the structure and dynamics of the outer plasmasphere using multiple geosynchronous satellites, *J. Geophys. Res.*, *99*(A6), 1147511481, doi:10.1029/93JA03526.

247 Phan, T. D., et al. (2000), Extended magnetic reconnection at the Earth's magnetopause
248 from detection of bi-directional jets, *Nature*, *404*, 848850, doi:10.1038/35009050.
249 Phan, T. D., B. U. Sonnerup, and R. P. Lin (2001), Fluid and kinetics signatures of
250 reconnection at the dawn tail magnetopause: Wind observations, *J. Geophys. Res.*,
251 *106*(A11), 2548925501, doi:10.1029/2001JA900054.
252 Spasojević, M., J. Goldstein, D. L. Carpenter, U. S. Inan, B. R. Sandel, M. B. Moldwin,
253 and B. W. Reinisch (2003), Global response of the plasmasphere to a geomagnetic
254 disturbance, J. Geophys. Res., 108(A9), 1340, doi:10.1029/2003JA009987.
255 Sonnerup, B. U. Ö, and L. J. Cahill Jr. (1967), Magnetopause structure and
256 attitude from Explorer 12 observations, *J. Geophys. Res.*, *72*(1), 171–183,
257 doi:10.1029/JZ072i001p00171.
258 Su, Y.-J., J. E. Borovsky, M. F. Thomsen, R. C. Elphic, and D. J. McComas (2000),
259 Plasmaspheric material at the reconnecting magnetopause, *J. Geophys. Res.*, *105*(A4),
260 7591–7600, doi:10.1029/1999JA000266.
261 Sweet, P. A. (1958), The neutral point theory of solar flares, in *Electromagnetic Phenom-*
262 *ena in Cosmical Physics*, edited by B. Lehnert, p. 123, Cambridge Univ. Press, New
263 York.
264 Trenchi, L., M. F. Marcucci, G. Pallocchia, G. Consolini, M. B. Bavassano Cattaneo,
265 A. M. Di Lellis, H. Reḿe, L. Kistler, C. M. Carr, and J. B. Cao (2008), Occurrence of
266 reconnection jets at the dayside magnetopause: Double Star observations, *J. Geophys.*
267 *Res.*, *113*, A07S10, doi:10.1029/2007JA012774.

Walsh, B. M., D. G. Sibeck, Y. Nishimura, and V. Angelopoulos (2013), Statistical analysis of the plasmaspheric plume at the magnetopause, *J. Geophys. Res.*, *118*, doi:10.1002/jgra.50458.

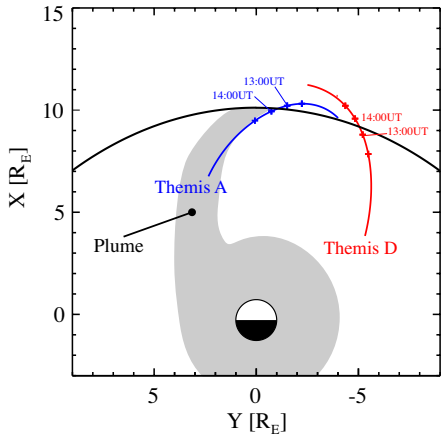

Figure 1. The locations of ThA (blue) and ThD (red) on 15 Sept 2008 in GSM. The grey region is a nominal location of the plasmasphere and plume.

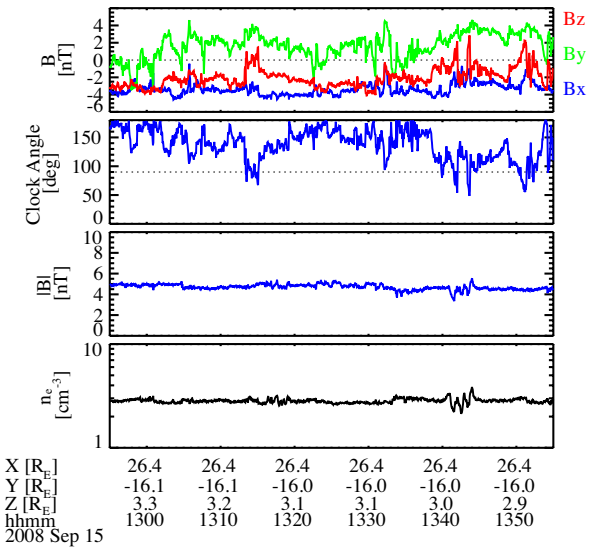

Figure 2. Upstream solar wind measurements from ThB. The spacecraft is just upstream of the bow shock at (X, Y, Z) = (26, -13, 3) R_E. From top to bottom the panels are magnetic field vector, IMF clock angle, magnetic field magnitude, and electron density.

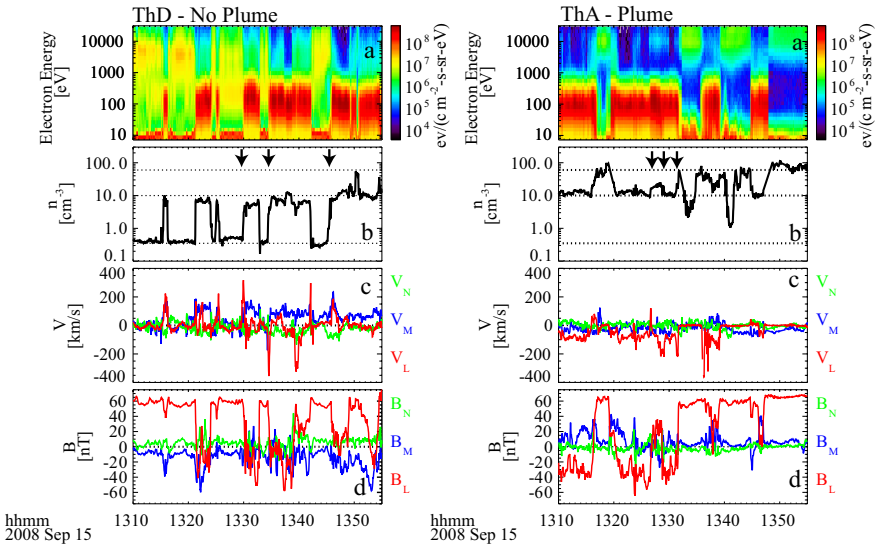

Figure 3. THEMIS measurements for the same time period (13:10-13:55 UT) are shown for ThD (left) and ThA (right). From top to bottom the panels are electron energy spectra, electron density derived from spacecraft potential, bulk flow components, and magnetic field components. Both spacecraft cross the magnetopause a number of times during the interval. The black arrows indicate boundary crossings with reconnection.

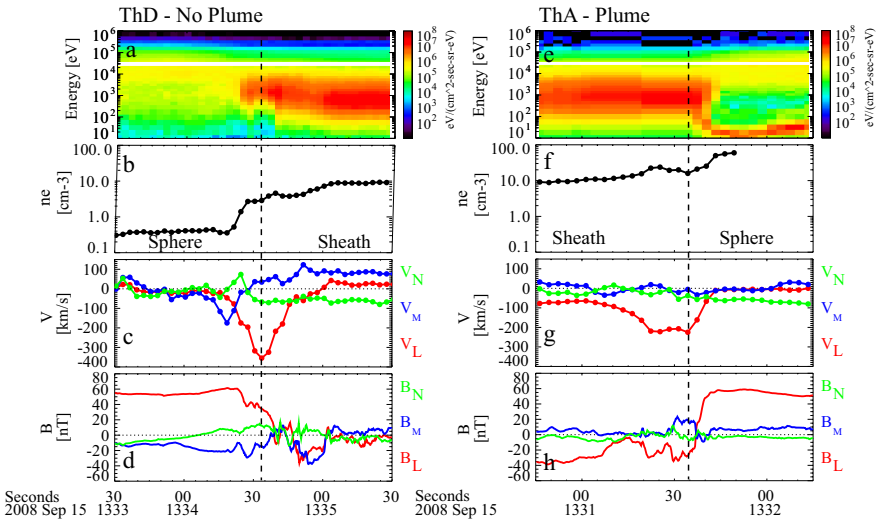

Figure 4. Magnetopause crossing from ThD (left) and ThA (right). From top to bottom the panels are ion energy spectragram, electron density derived from spacecraft potential, bulk flow components, and magnetic field components. The magnetic field and bulk flow are in boundary normal coordinates determined through MVAB. The vertical dashed bars indicate the time of the peak jet velocity.

Table 1. Parameters for reconnection measurements. "SC" is the THEMIS spacecraft. v_{C+S} is the calculated Cassak and Shay hybrid Alfvén velocity. The subscript m indicates magnetospheric side while s is the magnetosheath side. The ratio of magnetosphere to magnetosheath mass inflow is $\frac{n_m B_s}{n_s B_m}$. "Jet Field" is the orientation of the magnetic field vector at the time of the maximum jet velocity. A field orientation with $+B_L$ is magnetospheric while -B_L is magnetosheath for this event.

Time hh:mm	SC	v_{jet} [km/s]	v_{C+S} [km/s]	n_{jet} [cm^{-3}]	n_s [cm^{-3}]	n_m [cm^{-3}]	B_s [nT]	B_m [nT]	Mass inflow ratio	Jet Field
13:29	D	363	441	1.7	4.2	0.5	21	63	0.04	'sphere
13:34	D	362	364	2.9	8.4	0.4	24	63	0.05	'sphere
13:44	D	255	283	7.2	11.9	0.7	23	54	0.04	'sphere
13:26	A	190	213	15.2	9.8	20.3	51	29	2.35	'sheath
13:28	A	126	163	14.9	11.6	18.3	30	28	1.69	'sheath
13:31	A	221	176	15.9	9.4	55.0	38	56	3.97	'sheath